Science of Sintering, **54** (2022) 321-334

https://doi.org/10.2298/SOS2203321M

UDK: 666.112.3; 620.181.4

The Analysis of the Nucleation Process of the Lithium Germanium Phosphate Glass

Srdjan D. Matijašević[1*)], Snežana R. Grujić[2], Jelena D. Nikolić[1],Vladimir S. Topalović[1], Veljko V. Savić[1], Snežana N. Zildžović[1], Nebojša J. Labus[3]

[1]Institute for Technology of Nuclear and Other Mineral Raw Materials (ITNMS), 86 Franchet d Esperey, 11000 Belgrade, Serbia

[2]Faculty of Technology and Metallurgy, University of Belgrade, 4 Karnegijeva, 11000 Belgrade, Serbia

[3]Institute of Technical Sciences of SASA, Knez-Mihailova 35/IV, 11000 Belgrade, Serbia

Abstract:

The nucleation process of lithium germanium-phosphate glass was studied to determine the temperature range of nucleation and the temperature of the maximum nucleation rate. The differential thermal analysis (DTA), and scanning electron microscope (SEM) were used to reveal the nonisothermal and isothermal process of nucleation, respectively. The crystallization process occurred at a high homogeneous nucleation rate and the spherulitic crystal growth morphology. Nanostructured samples were obtained.

Keywords*: Lithium germanium-phosphate glass; Nucleation; DTA; SEM;*

1. Introduction

Solid lithium-ion conductors continue to attract great interest, especially for application in high energy density batteries and other electrochemical devices [1,2]. Based on conducting properties one of the most promising materials for such purpose is the glass-ceramics prepared from $Li_2O–Al_2O_3–GeO_2–P_2O_5$ glassy system. These materials can be obtained by the classic powder sintering route, sol-gel method, and common glass-ceramic processes [3,4].

The glass with the $22.5Li_2O·10Al_2O_3·30GeO_2·37.5P_2O_5$ (mol%) composition was chosen due to the possibility of obtaining a NASICON structure as the single phase with controlled crystallization [5].

These NASICON compounds have general formula $M(A_2B_3O_{12})$, where M is an alkali ion or alkaline earth ion, A is generally metal with a valence of 4 or more but is also substitutable by trivalent elements and B is often phosphorous but can be partially substituted by Si or As. They belong to a class of structurally isomorphous 3D framework compounds possessing high conductivity, often comparable to that of liquid electrolytes at higher temperatures. The high ionic conductivity of these materials is used in making devices such as membranes, fuel cells, and gas sensors [6]. In addition, their low thermal expansion coefficient value, fairly large surface area and ability to accommodate ions in the lattice make them a good host for radioactive waste, also promising used as catalyst supports. All these uses and remarkable properties justify the effort of their investigation.

*) **Corresponding author:** s.matijasevic@itnms.ac.rs

They generally crystallize in rhombohedral R3c space group related to open structures and the monovalent cation can easily migrate in lattice with low activation energy [7]. These materials are usually obtained by the powder sintering route and the crystallization of these glasses [8,9]. This method requires the knowledge of nucleation, crystallization, and crystal growth [10-12]. The aim of the present study is the investigation of the nucleation of germanium phosphate glass under no isothermal and isothermal conditions.

2. Materials and Experimental Procedures

Efforts were made to minimize impurity levels in the glass by careful choice of starting materials due to possible effects of the impurities on the nucleation rates [13]. The glass was prepared by melting a homogeneous mixture of reagent-grade (99.99 %) Li_2CO_3, Al_2O_3, GeO_2, and $(NH_4)_2HPO_4$ in a covered platinum crucible. The components were thoroughly mixed together and heated stepwise up to 300^{o}C to remove volatile substances. The melting was performed in an electric furnace CARBOLITE BLF 17/3 at T=1400^{o}C during t = 0.5 h. The melt was then quenched and pressed between steel plates and cooled in the air.

2.1 Chemical analysis

The chemical analysis was performed using spectrophotometer AAS PERKIN ELMER Analyst 300. The method of atomic absorption spectrophotometry (AAS) was used to determine the content of oxides, Li_2O, GeO_2, P_2O_5, Al_2O_3 in glass, after the dissolution of the sample in NaOH, and the composition was determined by analyzing the content of their cations in the solution. The measurement uncertainty was 0.49 %.

2.2 X-ray diffraction analysis

X-ray diffraction (XRD) was employed to identify and characterize crystalline phases released during heat treatment of glass samples at crystallization peak temperatures. The PHILIPS PW 1710 automatic diffractometer with the following characteristics was used for measurement: - X-ray tube Cu LFF 40 kW; 32 mA; - graphite monochromator and proportional counter with xenon; - recording area (2θ) from 4 to 70° (- scan time from 0 to 5 s). The intensities of diffracted CuKα1 X-rays (λ = 0.154060 nm) were measured at room temperature. The standard database (JCPDS database) for XRD patterns was used for phase identification. The results of the XRD test made it possible to determine the type and number of crystalline phases, as well as their quantitative ratio in the crystallized samples.

2.3 Differential-thermal analysis

The behavior of the glass during heating was monitored using DTA, on a DTA/TGA device NETZSCH STA 409EP under the following conditions: particle size of glass powder (0.5-0.65 mm), sample weight 100 mg, temperature measuring range from T = 20 – 800^{o}C, sample heating rate β = 10 ^{o}Cmin^{-1}, Al_2O_3 was used as a reference substance in a static air atmosphere. Glass powder for analysis was prepared by manual grinding of compact glass samples in an agate mortar and sieving on a standard series of sieves. Before the DTA experiments, the device was calibrated with quartz of standard purity 99.995 % with known crystallization temperature. The characteristic temperatures of the tested glasses were determined from the DTA curve.

2.4 Scanning electron microscope (SEM)

The surface and fractures (fracture surfaces) of the crystallized samples were analyzed by SEM MIRA3 XMU. The MIRA 3 XMU scanning electron microscope uses a high-brightness Schottky emitter with high contrast and resolution of up to 1.0 nm at 30 kV and with a magnification up to 10^6 times. The large chamber (250 mm) can operate in low and high vacuum mode from 150 Pa to < 9 x 10^{-3} Pa pressure. The recording of the sample surface is in stereoscopic 3D mode with the possibility of a high sampling speed of up to 20 ns/pixel. All samples were coated in gold on a JEOL JFC 1100 sputter-coater before analysis. The SEM results were used to determine the crystallization mechanism, crystal growth morphology and kinetics of the isothermal crystallization process.

2.5 Experiment of crystallization of glass under nonisothermal and isothermal conditions

Tests of glass crystallization processes were performed under nonisothermal and isothermal conditions. Before the $22.5Li_2O{\cdot}10Al_2O_3{\cdot}30GeO_2{\cdot}37.5P_2O_5$ (LAGP) composition tests were done, experiments were performed to obtain the data necessary for the application of the classical theory of nucleation (CNT) for calculating the nucleation rate as well as for calculating the surface energy.

2.6 Crystallization of glass under nonisothermal conditions

To determine the temperature range of nucleation and the temperature of the maximum nucleation rate, granulation samples of g_r = 0.50-0.65 mm and constant mass m = 100 mg were used, which were heated at a rate of β=10 $^oCmin^{-1}$ during the DTA experiment. Before DTA measurements, the samples were heat-treated at the selected nucleation temperature for different times t_n = 15, 30, 60, 120, 180, and 300 mins to obtain a complete nucleation curve. Nucleation temperatures were from T = 500-620^{o}C with a step of 10 $^oCmin^{-1}$ [14].

2.7 Crystallization of glass under isothermal conditions

For isothermal crystallization experiments, compact samples of the glass with suitable dimensions were used, which were heated in an electric furnace CARBOLITE CWF 13/13 with a heating rate regulator and a temperature accuracy of ± 1^{o}C.

Tab. I Exp. conditions for testing the isothermal nucleation of compact samples of glass.

T_n[^{o}C]	t_n [h]									
510	4	6	7	18	20	24	26	28	30	/
520	1	2	3	4	5	6	7	8	9	9.5
535	1	2	3	4	4.5	5	5.5	/	/	/
550	1	2	3	4	5	8	24	/	/	/
565	0.5	0.45	1	/	/	/	/	/	/	/

Samples of LAGP glass were placed on platinum plates and heated at a rate of β = 10 $^oCmin^{-1}$ (Tab. I). The temperature range of crystallization was previously determined on DTA. Upon reaching the selected nucleation and crystallization temperature, the samples were isothermally heated for a time of 30 min to 30 h. After the crystallization completed, the samples were taken out of the furnace, and then partly prepared in the form of XRD sample powder, and partly in the form of compact pieces of suitable fractures for SEM. The SEM was

used to analyze the microstructure of the glass samples and the results were used to determine the crystallization mechanism, crystal growth morphology and kinetics of the isothermal crystallization process. Tab. I, shows the experimental conditions for the nucleation of compact glass samples - nucleation temperature T_n and nucleation time t_n.

The nucleation process of the test glass can be analyzed by monitoring the nucleation process during continuous heating of the test sample (non-isothermal) and/or observing the process during time *t*, at the selected nucleation temperature (isothermal).

3. Results and Discussion

The glass mixture for obtaining the selected glass composition was melted in an electric furnace. The resulting melts were poured between two steel plates and cooled in the air. During cooling, the melt solidified into a transparent, homogeneous, and colorless glass. The XRD analysis revealed the quenched melts to be vitreous (figure not shown). The results of the chemical analysis show that a glass composition of 22.5 Li_2O·10 Al_2O_3·30 GeO_2·37.5 P_2O_5 (mol%) (LAGP) was obtained.

3.1. Nonisothermal analysis of temperature range of nucleation and temperature of maximum glass nucleation rate for tested glass

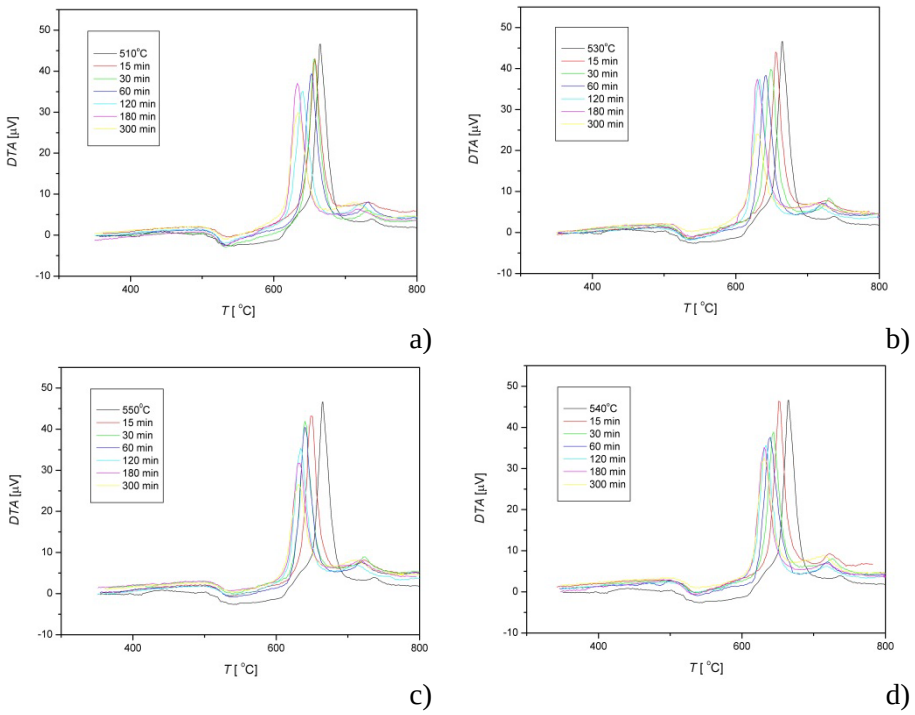

Fig. 1. Crystallization peaks temperature T_p, dependence on heat treatment time: a) T_n = 510°C, b) T_n = 530°C, c) T_n = 540°C, d) T_n = 550°C.

To determine the temperature range of nucleation and the temperature of the maximum nucleation rate, the analysis of changes in sample parameters read from the DTA (crystallization exothermic maximum, T_p and crystallization peak height in Celsius [°C]), $(\delta T)_p$, depending on the nucleation temperature T_n) have been performed. The procedure involves nucleating a glass sample at a selected temperature T_n during time t_n (isothermal

heating), then heating the sample non-isothermally at a certain rate β (e.g. 10 ^{o}Cmin^{-1}) and monitoring the change in temperature and *exo* maximum height on the DTA device. The procedure is then repeated at a different nucleation temperature, but with the same heat treatment time, granulation and mass of the test sample. In this way, the number of nuclei formed in the glass during the DTA assay is kept low and is similar for all samples during the experiment. The change in the number of nuclei in the sample is a consequence of the discrete property of the sample itself, i.e. the nucleation rates are different at different temperatures. The procedure is then repeated under the same experimental conditions, changing the heat treatment temperatures. It should be noted that for this determination it is sufficient to report the mentioned experiments for one time of heat treatment. From the crystallization peak (exothermic maximum) of the previously heat-treated glass at the selected temperature over time, the values $(\delta T)_p$, $T_p^{-1,}$ and ΔT_p (difference in the temperature of the crystallization peak of the heat-nontreated and heat-treated sample) depending on the heat-treatment time are obtained.

During the analysis of the phase composition and the crystallization mechanism, of the four-component LAGP glass, XRD analyses revealed that this glass crystallizes polymorphic, which provides the possibility of using a non-isothermal method to study the nucleation process [15].

Fig. 1 presents DTA diagrams for samples that were heat-treated for different times (15-300 minutes) at the same nucleation temperature before the DTA experiment.
It can be seen that the time of the heat treatment affects the left shifts of the peaks and peak reduction. The values of $(\delta T)_p$, and $T_{p,}$ of the crystallization peaks of the heat-treated samples of LAGP composition are shown in Figs. 2 and 3, respectively.

Fig. 2 graphically shows the dependence $(\delta T)_p$ on the nucleation temperature T_n for different heat treatment times of the sample.

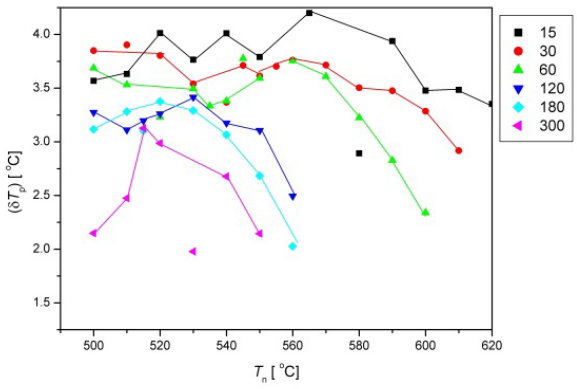

Fig. 2. Parameter $(\delta T)_p$, dependence on nucleation temperature T_n for different heat treatment times (15-300 min) for LAGP glass.

The dependence of the height of the crystallization peaks on the nucleation temperature increases irregularly, reaching a maximum. The shape of the dependence curves $(\delta T)_p$ as a function of T_n (Fig. 2) indicates the possibility that nucleation and crystal growth occur simultaneously in the observed LAGP glass in the examined temperature range, or a pronounced dependence of the nucleation rate on time. This possibility is indicated by a different form of dependence $(\delta T)_p$ in relation to the dependence of T_p^{-1} on the heat treatment temperature (Fig. 3). The heights of the crystallization peaks decrease with the time of heat treatment. During heat treatment at temperature T_n, part of the sample crystallizes, which represents a decrease in the number of nuclei present for crystallization and leads to a decrease in the height of the crystallization peak during DTA experiments. The dependence of

the reciprocal value of the crystallization peak temperature T_p^{-1} of the previously heat-treated sample at different nucleation temperatures (T_n) during the heat treatment time (t_n) is shown in Fig. 3.

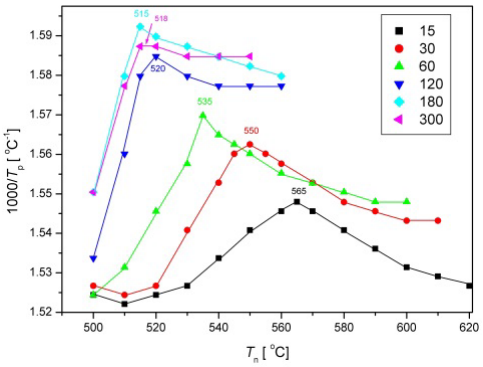

Fig. 3. T_p^{-1} vs. T_n for different heat treatment times (15-300 min) for LAGP composition.

It is noticed (Fig. 3) that the temperature dependence of T_p^{-1} increases, reaching a maximum, and then decreases, describing the characteristic shape of "bells" for glass.

Tab. II, shows the maximum values of the parameters T_p^{-1}, ΔT_p and (δT) at the nucleation temperature T_n max as a function of f (T, t) for the LAGP composition.

Tab. II Max. nucleation temperatures as a function of temperature and heat treatment time.

f(T,t)	T_p^{-1}	ΔT_p	$(\delta T)_p$
180	1.5923	37	3.375
300	1.5873	35	3.127
120	1.5848	34	3.416
60	1.5618	28	3.777
30	1.5625	25	3.804
15	1.5480	19	4.199

From the given table, it can be noticed that with the increase of temperature and heat treatment time, the crystallization peaks move towards to lower temperatures, the temperature difference between the peaks decreases (ΔT_p) and the peak height decreases $(\delta T)_p$ due to heat treatment (samples nucleation). It can be showed the reciprocal values of the maximum of crystallization peaks T_p^{-1} of previously heat-treated samples at all nucleation temperatures T_n over time, (Fig. 4).

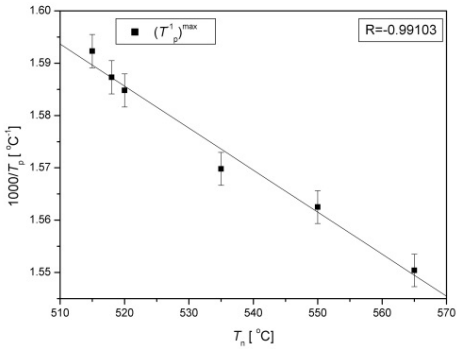

Fig. 4. $1000/T_p^{-1}$ vs. T_n for different heat treatment times of LAGP composition.

It can be seen (Fig. 4) that the dependence of the maximum T_p^{-1} as a function of T_n can be represented by a line of the form Y = 2.00324+(– 8.0311·10^{-4}·X) for the LAGP composition, indicating homogeneous nucleation.

3.2. Isothermal analysis of the nucleation process of the tested glasses

Bulk glass samples heated at a constant rate of β = 10 ^{o}Cmin^{-1} to the nucleation temperature at which they were kept for a specific time (0.5-30 h) in an electric furnace, were used to examine the glass crystallization under isothermal conditions. The experimental conditions for crystallization of compact glass samples are shown in Tab. I (Materials and methods). Heat-treated samples were analyzed using SEM and XRD methods. The results of SEM analysis made it possible to determine the mechanism of glass crystallization, crystal growth morphology, crystal growth rate and nucleation and its temperature dependence.

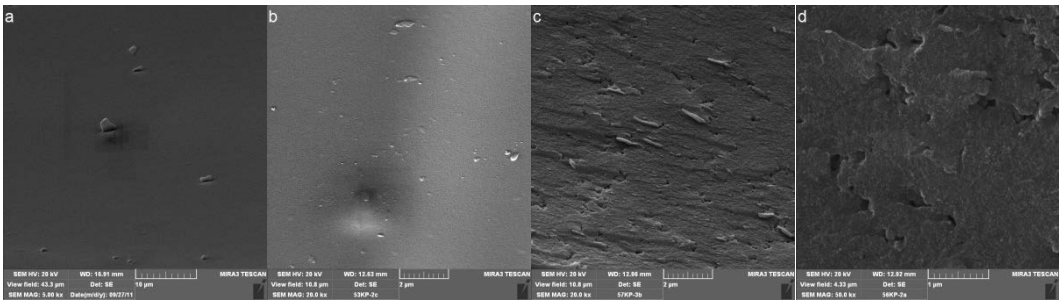

Fig. 5. SEM micrograph of glass treated at nucleation temperature T = 510 ^{o}C during a) t = 7 h, b) 18 h, c) 26 h and d) 30 h.

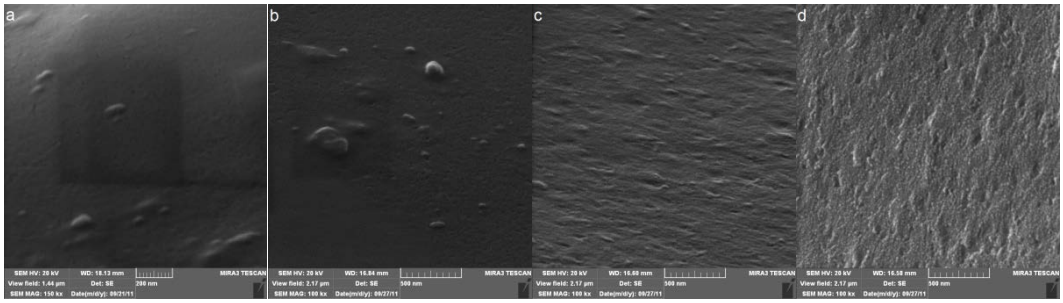

Fig. 6. SEM micrograph of glass treated at nucleation temperature T = 520 ^{o}C during a) t = 2 h, b) 6 h, c) 7 h and d) 8 h.

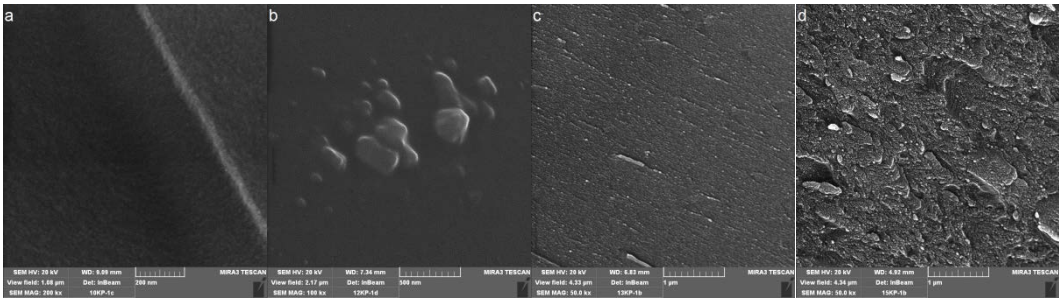

Fig. 7. SEM micrograph of glass treated at nucleation temperature T = 535 ^{o}C during a) t = 1 h, b) 3 h, c) 4 h and d) 5 h.

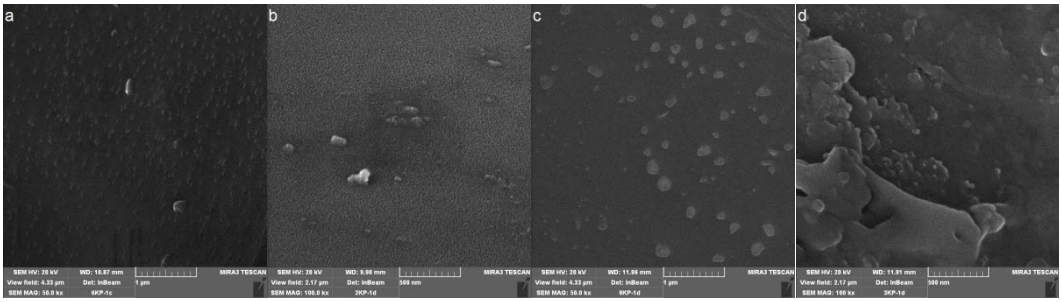

Fig. 8. SEM micrograph of the treated glass at nucleation temperature T = 550 ^{o}C during a) t = 2 h, b) 3 h, c) 4 h and d) 8 h.

The phase composition of the tested glass was determined based on Ritveld's analysis [16]. Polymorphic crystallization of glass with crystalline phase $LiGe_2(PO_4)_3$ was ascertained. Nucleations of the $LiGe_2(PO_4)_3$ phase were examined by SEM analysis.

It can be noticed (Fig. 5-8) how the size and density of the crystals increase with the time of heat treatment (a-d).

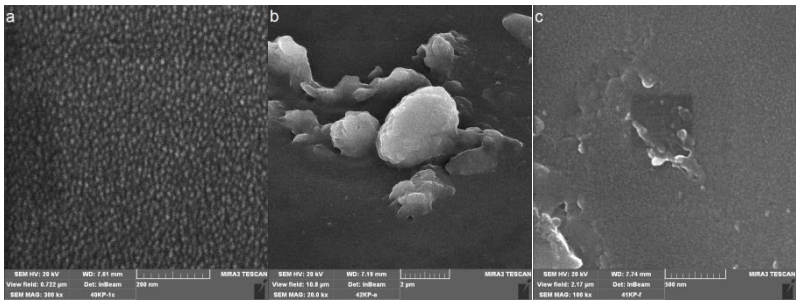

Fig. 9. SEM micrograph of the treated glass at nucleation temperature T = 565^{o}C during a) t = 30 min, b) 45 min, and c) 60 min.

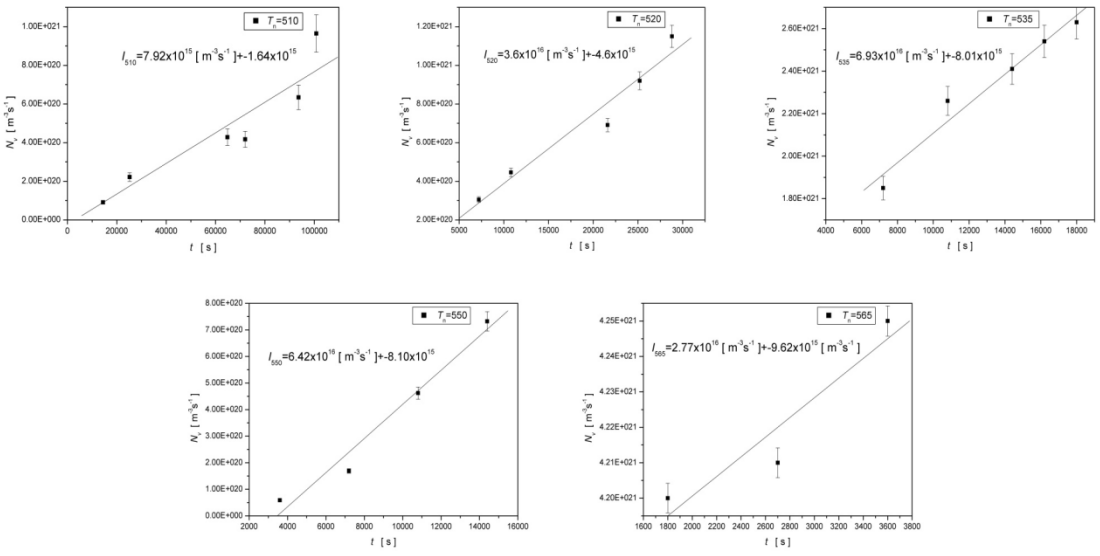

Fig.10. N_v dependence on the heat treatment time at the nucleation temperatures of crystals in LAGP glass at a) 510, b) 520, c) 535, d) 550 and e) 565^{o}C, respectively

The results shown in Figs. 5-9 indicate that the morphology of crystal growth in glass is spherical in nature. In Figs. 6b, 7b, and 8b, the spherical crystals of dimensions below 150 nm can be seen.

Fig. 10 shows the dependences of the number of nuclei per unit volume (N_v) on the time (t) of heat treatment at nucleation temperatures (510, 520, 535, 550 and 565°C). Crystal nucleation rates in LAGP glass for each nucleation temperature were determined from the slope of the linear functions.

Tab. III, shows the nucleation rates of the LAGP composition at different temperatures, determined by the isothermal method.

Tab. III Nucleation rates (I) at different temperatures T_n.

Ordinal number	T_n [°C]	I [$m^{-3}s^{-1}$]
1	510	$7.92 \cdot 10^{15}$
2	520	$3.60 \cdot 10^{16}$
3	535	$6.93 \cdot 10^{16}$
4	550	$6.42 \cdot 10^{16}$
5	565	$2.77 \cdot 10^{16}$

Based on the obtained results, the dependence of the crystal nucleation rate on the temperature in LAGP glass was determined experimentally.

Experimentally determined nucleation rates were used to verify the applicability of the classical nucleation theory (CNT) during the monitoring of the glass nucleation process of the LAGP composition in the temperature range 510-565°C. According to the classical theory of nucleation, the steady-state nucleation rate (I_o) can be calculated using Eq. (1) [17,18]:

$$I = \left[\frac{A_c \cdot T}{\eta} \right] \exp\left(- \frac{W^*}{kT} \right) \qquad (1)$$

the factor $A_c = n_v k / 3\pi\lambda^3$; n_v - number of homogeneous nucleation sites per unit volume, W^*- thermodynamic barrier for nucleation, η-viscosity value; k - Boltzmann's constant; T - temperature; λ - is the characteristic size parameter of the structural units;
also for spherical nuclei:

$$W^* = \frac{16\pi \cdot V_m^{\ 2} \cdot \sigma^3}{3 \cdot \Delta G^2} \qquad (2)$$

here is V_m - the molar volume of the crystalline phase; σ - surface energy of the crystal/liquid interface; ΔG - the thermodynamic driving force for the glass to crystal transformation (change in free energy of liquid / solid phase transformation).
Combining Eqs. (1) and (2), the nucleation rate is given by:

$$I = \left[\frac{n_v \cdot k \cdot T}{3 \cdot \pi \cdot \lambda^3 \cdot \eta} \right] \exp\left(- \frac{16 \cdot \pi \cdot V_m^{\ 2} \cdot \sigma^3}{3 \cdot k} \cdot \frac{1}{\Delta G^2 \cdot T} \right) \qquad (3)$$

Eq. (3) provide the possibility of constructing a diagram showing the dependence ln ($I\eta/T$) in a function ($1/\Delta G^2 T$), should be a straight line so that the surface energy σ can be determined from the slope of the line, and the pre-exponential factor A_c from the intercept of the ordinate axis.

Assumptions for the application of the classical theory of nucleation are that the composition of the crystal phase and glass is the same, ie. that the system is homogeneous, that the resulting embryos are spherical in shape, that they have the same composition as the parent (macro) phase and that the surface energy at the crystal-melt interface does not depend on the temperature and diameter of the nucleus, σ_∞, ie that it is constant. If these conditions are fulfilled, then from Eq. (3) the dependence ln ($I_{(exp)}\cdot\eta$ /T) of 1/ ($T\cdot\Delta G^2$) is obtained, which should be linear. The construction of the diagram can determine the surface energy σ_∞ from the slope of the line, and the pre-exponential constant A_c from the segment on the ordinate axis. The experimentally determined rates of stationary nucleation are given in Tab. III, the corresponding values of viscosity (η), molar volume (V_m), and crystallization energy [19], based on which the linear dependence in Fig. 11 was calculated and obtained.

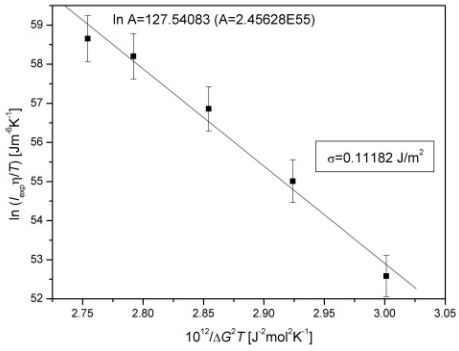

Fig. 11. Dependence of ln ($I_{ex}\cdot\eta/T$) of 1 / ($T\cdot\Delta G^2$) for LAGP glass.

Based on the diagram (Fig. 11), the surface energy σ_∞ = (0.112±0.008) Jm^{-2} was calculated, as well as the pre-exponential factor $A_{c(exp)}$ ~ ($2.46\cdot10^{55}$ ±$1.77\cdot10^{2}$) $Jm^{-6}K^{-1}$ by the slope and intercept, respectively. The determined value of the pre-exponential factor A_c is 27 orders of magnitude higher than the calculated theoretical value A_c = $1.935\cdot10^{28}$ $Jm^{-6}K^{-1}$. This discrepancy is not uncommon between experimental and theoretical values [20,21]. Based on the calculated surface energy (σ_∞) at the crystal-liquid interface and from the ratio [22-24]:

$$\sigma = \alpha\cdot\Delta H_m\cdot V_m^{-2/3}\cdot N_A^{-1/3} \qquad (4)$$

where: α-empirical coefficient, a non-dimensional parameter, N_A-Avogadro's number; the value of the non-dimensional parameter (α) can be calculated. For the tested four-component glass, α_{lgp}=0.384. This result represents the lower limit in the case of homogeneous nucleation in super-cooled liquids (for silicate glasses) (0.40-0.55) [25,26]. A non-dimensional parameter is an empirical coefficient whose value is less than 1, as a consequence of the state that atoms on the surface have fewer adjacent atoms than those in volume. For lower values of the α coefficient, lower thermodynamic barriers for nucleation and higher nucleation rates are expected, provided that the kinetic barrier for nucleation is not large. The relatively small value of the surface energy at the crystal/liquid boundary and the lower value of the empirical coefficient could indicate a smaller difference in the structure of the crystal phase and the starting glass (polymorphic transformation). Nucleation rates determined experimentally at different temperatures (Tab. III), the corresponding values of viscosity, free energy change, molar volume, and the theoretical value of the pre-exponential factor (A_c) (Eq. 1) were used to calculate the surface energy value of the crystal/liquid interface depending on temperatures (Eqs. 3 and 4).

Fig. 12, shows the calculated dependence of surface energy on temperature, which can be represented by the expression $\sigma_{(T)} = -0.05124+(1.98958\cdot10^{-4}\cdot T)$, [$Jm^{-2}$], where the temperature (T) given in degrees Celsius [^oC].

From the figure, it can be noticed that the surface energy increases with increasing temperature in steps of $d\sigma/dT = 0.199\cdot10^{-3}$ $Jm^{-2o}C^{-1}$ in the temperature range of T=510-565^{o}C. The value of the increase in surface energy depending on the temperature obtained in this way was also found in other glasses [26,27]. The obtained values of surface energy at different temperatures were used to calculate the theoretical nucleation rates (according to Eqs. 1-3), other parameters necessary for the calculation are given in Tab. IV.

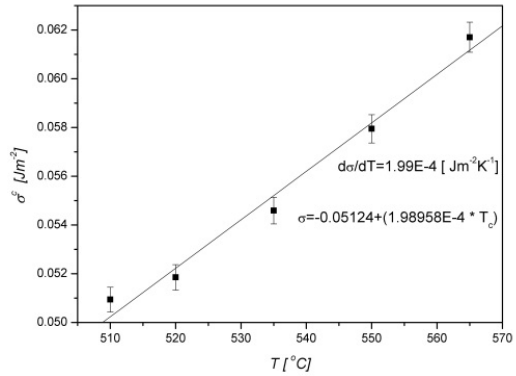

Fig. 12. Dependence of the calculated surface energy of the crystal/melt boundary (σ_T) on the temperature T for LAGP glass.

Tab. IV Parameters for calculating the n rate and crystal growth [15,19].

$k = 1.380622\cdot10^{-23}$ J K^{-1}	A = - 2.8361
$l_{P\text{-}O} = 1.58\cdot10^{-10}$ m	B = 3430.60
$\lambda = 20.5696\cdot10^{-10}$ m	T_o = 555.8459 [K]
T_m = 1368.65 K	ΔS_m = 44.08 J mol^{-1} K^{-1}
ΔH_m =60.325 $kJmol^{-1}$	$V_m = 121.09\cdot10^{-6}$ m^3mol^{-1}

Fig. 13 shows a nucleation rate comparative dependence on temperature, (I_{teor}) calculated with a constant value of surface energy σ_∞ (Fig. 11), with a variable value of σ_T as a function of temperature (Fig. 12) and experimentally determined values of I_{exp} (Tab. II, Fig. 13).

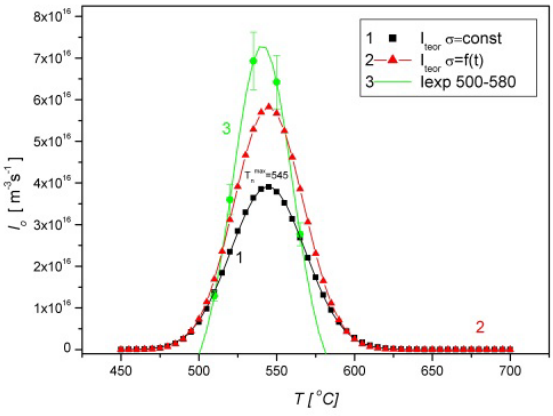

Fig. 13. I_{teor} nucleation rate in relation to I_{exp} on the temperature in LAGP glass.

The dependence is shown graphically (Fig. 13) and has the characteristic shape of a "bell". The temperature of the maximum nucleation rate (I_{exp} = 7.34·10^{16} m^{-3}s^{-1}), determined based on isothermal experiments, is T_{Nmax} = (541±5)^{o}C (Fig. 13, curve 3). It can be noticed that the nucleation rates at given temperatures increase, reaching the maximum T_{Nmax}, this value is determined graphically (Fig. 13), and then decrease. The LAGP composition has a very high nucleation rate compared to hitherto known inorganic glass systems [28-30]. The obtained experimental values of I_{exp} nucleation rate (curve 3) are slightly higher in relation to the theoretical values of I_{teor} rate (curves 1 and 2). Better agreement of experimental and theoretical values was obtained by applying variable values of surface energy depending on temperature (curve 2) during the calculation in Eqs. (1-3). The calculated values of temperature T_{Nmax} = 545^{o}C of the maximum rate of stationary nucleation (I_{teo} = 5.83·10^{16} m^{-3}s^{-1}) show very good agreement with the experimentally determined T = 541^{o}C. The previous finding that CNT gives a good description of temperature dependence of the steady-state nucleation rate (I_o) is also shown here. The high nucleation rates (I), of the four-component glass composition ~ 10^{16} m^{3}s^{-1} in the examined temperature range T = 510-565^{o}C are related to the small values of the kinetic and thermodynamic barrier because the growth process of the crystal phase of glass is determined by phase boundary processes. The melting entropy of the tested glass is ΔS_m = 44.08 Jmol^{-1}K^{-1} [15]. Based on this value, which is greater than 4R [31,32], the entropy change can be considered as large and the crystal growth process can be described as - growth at the “smooth” boundary by a spiral screw dislocation model.

4. Conclusion

The glass 22.5Li_2O·10Al_2O_3·30GeO_2·37.5P_2O_5 (LAGP) was obtained by standard melt-quenching technique. LAGP glass nucleations were examined by DTA, and SEM analysis. The presented results indicate that the morphology of crystal growth in glass is spherulite in nature and that it is controlled by phase boundary reactions.

The constant value of the surface energy σ_∞ = 0.112 Jm^{-2} was calculated, as well as the pre-exponential factor $A_{c\ (exp)}$ ~ 2.46·10^{55} Jm^{-6}K^{-1}. The dependence of surface energy on temperature is represented by the expression: $\sigma_{(T)}$ = – 0.05124+ (1.99·10^{-4}·T) [J·m^{-2}], T [^{o}C]. The value of the increase in surface energy depending on the temperature obtained in this way was also found in other glasses. The empirical coefficient for the tested glass was α_{lgp} = 0.384. The maximum rate of stationary nucleation of $LiGe_2(PO_4)_3$ phases was calculated and is I_{teo} = 5.83·10^{16} m^{-3}s^{-1} at T_{Nmax} = 545^{o}C. The high nucleation rates of the four-component glass composition ~ 10^{16} m^{3}s^{-1} in the examined temperature range T = 510-565^{o}C are related to the small values of the kinetic and thermodynamic barrier because the growth process of the crystal phase of glass is determined by processes at the phase boundary.

Acknowledgments

The authors are grateful to the Ministry of Education, Science and Technological Development of the Republic of Serbia for the financial support (grant contract No.: 451-03-9/2021-14/200023 and 451-03-68/2021-14/200135).

5. References

1. N. Anantharamulu, K. K. Rao, G. Rambabu, B. V. Kumar, V. Radha, M. Vithal, J. Mater.Sci., 46 (2011) 2821-2837.

2. Z. Zhang, Y. Shao, B. Lotsch, Y-S. Hu, H. Li, J. Janek, L.F. Nazar, C-W. Nan, J. Maier, M. Armand, L. Chen, Energy Environ. Sci., 11 (2018) 1945-1976.
3. J. W. Fergus, J. Power Sources, 195 (2010) 4554-4569.
4. H. Ma, C. Bao, Sci. Sinter., 53 (3) (2021) 387-395.
5. S. V. Pershinaa, E. A. Il'inaa, K. V. Druzhinina, A. S. Farlenkov, J.Non Cryst.Solids, 527 (2020) 119708.
6. P. Knauth, 180 (2009) 911-916.
7. F. Zheng, M. Kotobuki, S. Song, M. O. Lai, L. Lu, J. Power Sources, 389 (2018) 198-213.
8. A. M. Cruz, E. B. Ferreira, A. C. M. Rodrigues, J. Non Cryst. Solids, 355 (2009) 2295-2301.
9. J. N. Stojanović, S. V. Smiljanić, S. R. Grujić, P. J. Vulić, S. D. Matijašević, J. D. Nikolić, V. V. Savić, Sci. Sinter., 51 (4) (2019) 389-399.
10. K. F. Kelton, A. L. Greer, Nucleation in Condensed Matter: Applications in Materials and Biology, Pergamon, Amsterdam (2010).
11. J. W. P. Schmelzer, A. S.Abyzov, V. M. Fokin, C. Schick, E. D. Zanotto, J. Non Cryst.Solids, 429 (1) (2015) 24-32.
12. S. D. Matijašević, M. B. Tošić, S. R. Grujić, J. N. Stojanović, V. D. Živanović, J. D. Nikolić, Sci. Sinter., 43 (1) (2011) 47-53.
13. J. Maletaškić, B. Todorović, M. Gilić, M. Marinović-Cincović, K. Yoshida, A. Gubarevich, B. Matović, Sci. Sinter., 52 (1) (2020) 41-52.
14. S. D. Matijašević, S. R. Grujić, V. S. Topalović, J. D. Nikolić, S. V. Smiljanić, N. J. Labus, V. V. Savić, Sci. Sinter., 50 (2) (2018) 193-203.
15. S. D. Matijašević, V. S. Topalović, S. R. Grujić, V. V. Savić, J. D. Nikolić, N. J. Labus, S. N. Zildžović, Sci. Sinter., 53 (3) (2021) 301-310.
16. J. D. Nikolić, S. V. Smiljanjić, S. D. Matijašević, V. D. Živanović, M. B. Tošič, S. R. Grujić, J. N. Stojanović, Process. Appl. Ceram., **7** (4) (2013) 147-151.
17. P. F. James, J. Non- Cryst. Solids, 73 (1985) 517-540.
18. C. J. R. Gonzales Oliver, D. O. Russo, P. F. James, Phys.Chem. Glasess, 45 (2004) 100-106.
19. S. Matijašević, "Crystallization behaviour of multicomponent germanate glasses", doctoral dissertation, TMF, Belgrade, 2012.
20. S.Grujić, N. Blagojević, M. Tošić, V. Živanović, J. Nikolić, Ceram. Silikaty, 53 (2009) 128-136.
21. E. D. Zanotto, P. F. James, J. Non-Cryst.Solids, 74 (1985) 373-394.
22. D. Turnbull, J. Appl.Phys., 21 (1950) 1022-1028.
23. A. S. Skapski, *Acta Metall.*, 4 (1956) 576-582.
24. I. Gutzow, J. Schmelzer, The Vitreous State: Thermodynamics, Structure, Rheology and Crystallization, Springer, Berlin, 1995, p. 469.
25. K. Gupta, D. R. Cassar, E. D. Zanotto, J. Non-Cryst. Solids, 442 (2016) 34–39.
26. S. Manrich, E. D. Zanotto, Cerâmica, 41 (271) (1995) 105-109.
27. A. A. Cabral, V. M. Fokin, E. D. Zanotto, J. Non-Cryst.Solids, 343 (2004) 85-90.
28. V. M. Fokin, E. D. Zanotto, N. S. Yuritzyn, J.W.P. Schmelzer, J. Non-Cryst. Solids, 352 (2006) 2681-2714.
29. A. M. Kalinina, V. M. Fokin, V. N. Filipovich, J. Non-Cryst. Solids, 38-39 (1980) 723-728.
30. V. M. Fokin, E. D.Zanotto, J.W.P. Schmelzer, J. Non-Cryst. Solids, 321 (1-2) (2003) 52-65.
31. W. D. Kingery, H. K. Bowen, D. R. Uhlmann, Introduction to ceramics, Wiley-Interscience Publication, John Wiley and Sons, Inc, New York, 1976.
32. S. V. Smiljanić, S. R. Grujić, S. Matijašević, J. Stojanović, J. Nikolić, V. Savić, D. Ž. Popović, J. Therm. Anal. Calorim., 146 (4) (2021) 1569-1576.

Сажетак: *Одређена је температурна област нуклеације и температура максималне брзине нуклеације за одабрано литијум-германијум-фосфатно стакло. Диференцијална термичка анализа (ДТА) и скенирајући електронски микроскоп (СЕМ) су коришћени за одређивање особина неизотермног и изотермног процеса нуклеације, респективно. Процес кристализације се дешава при високој брзини хомогене нуклеације и сферулитној морфологији раста кристала. Добијени су наноструктурирани узорци.*
Кључне речи*: Литијум-германијум-фосфатно стакло, нуклеација, ДТА, СЕМ.*